ISBN: 978-3-95450-262-2 ISSN: 2673-5350 doi: 10.18429/JACoW-IBIC2025-TUPMO17

PHASE CONTRAST ISSUES OPERATING PINHOLE CAMERAS WITH LOW-EMITTANCE BEAMS

M. Labat*, A. Bence, P. Mercère, P. Dasilva, D. Pédeau, N. Hubert
Synchrotron SOLEIL, Gif-sur-Yvette, France

Abstract

In the framework of SOLEIL-II, the project of SOLEIL's storage ring upgrade towards lower emittances, preliminary studies were performed to pinpoint the resolution limits of the exisiting pinhole cameras. However, while reducing the vertical emittance from the SOLEIL's nominal 50 pm·rad value to 9 pm·rad, unexpected filaments were observed in the image plane of the pinhole cameras, severely spoiling the reliability of the emittance measurement. Investigations, on the existing pinhole cameras as well as on the Metrology beamline of SOLEIL, revealed that those filaments correspond to a phase contrast imaging of the UHV Aluminium window, located before the pinhole. In this work, we first report on experimental measurements performed to identify the origin of this issue and on our attempts of mitigation using a phase blurrer and testing different types of window.

INTRODUCTION

SOLEIL storage ring presently enables to store electron beams with an horizontal emittance of 3.9 nm·rad and a vertical emittance that can be varied from ≈ 7 up to 200 pm·rad. These emittances are measured by two pinhole cameras (PHC) [1, 2], one being used in a feedback loop to maintain the vertical emittance at 50 pm·rad ± 5 % during users' operation. However, on the forthcoming SOLEIL-II storage ring, these emittances will be significantly reduced. Relying on a multibend achromat lattice, the targetted emittances in operation are 85 pm·rad in the horizontal and 53 pm·rad in the vertical plane, with a vertical emittance at minimum coupling expected below 1 pm·rad. The existing PHCs can not resolve such low–emittances. This is why preliminary experiments were launched to anticipate a resolution improvment of our emittance diagnostics.

EXPERIMENTAL SETUP

The experimental setup of the PHCs [2] is shown in Fig 1. The X-ray content of the Synchrotron Radiation (SR) emitted by one of the ring dipoles (ANS-C02.D1 for PHC1 and ANS-C16.D2 for PHC3) is first extracted from the dipole vacuum chamber through a metallic UHV window. This window is made of Aluminium 6061 T6, an alloy widely used for vacuum components. The two main metals in addition to Aluminium (Z = 13) are Magnesium (Z = 12) about 1 % and Silicium (Z = 14) about 0.8 %. Relying on a parabolic shape, it is only 1 mm thick on the SR path while exhibiting a scratched exit surface (see Fig. 2). The SR then passes through a Copper filter of variable thickness (from 0 up to 2 mm) which enables to block the low energy photons. For emittance measurements (see Fig. 1a), a pinhole is inserted on the X-ray path. This pinhole is made of Tungsten blades defining a rectangular aperture of 15 × 10 µm. The SR finally hits a CdW04 scintillator of 0.5 mm thickness converting the X–rays into visible light. The intensity distribution of this visible light at the rear of the scintillator is then simply imaged on a CMOS camera with a pair of lenses. The ratio between the distance *D* from pinhole to scintillator, and the distance *d* from source point to pinhole sets the magnification of the pinhole. The pinhole can be removed from the X-ray path (see Fig. 1b). This configuration enables to observe the intensity distribution of the SR layer on the scintillator.

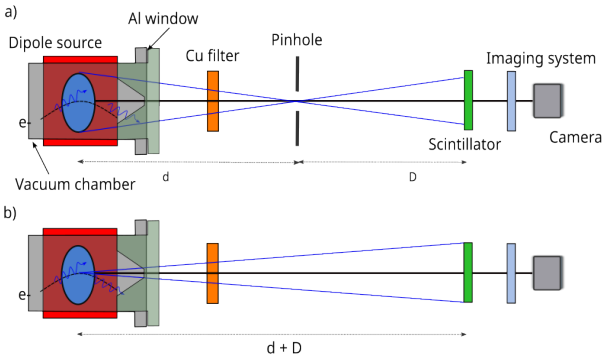

Figure 1: Experimental setup of the pinhole cameras installed at SOLEIL: a) with the pinhole imaging for emittance measurement, b) without pinhole for SR layer measurement.

PHASE–CONTRAST IMAGING ISSUE

Preliminary experiments on SOLEIL's PHCs aimed at finely compare measurements with SRW [3] simulations with low vertical emittances, for further extrapolation on improved resolutions. SOLEIL storage ring was therefore operated with a dedicated optics allowing to reach the minimum coupling, i.e. the minimum vertical emittance (≈ 7 pm·rad). In these conditions, it rapidly appeared that the emittance measurement was suffering from a strong dependency to the beam orbit. To understand this unexpected dependency, the pinhole was removed, revealing a high–contrast filamented pattern (see Fig. 3). These structures were observed simultaneously on the two PHCs. A scan of the pinhole transverse position confirmed that the emittance value was strongly correlated to the local intensity of the filamented SR, a correlation responsible for the beam orbit dependency previously observed.

* marie.labat@synchrotron-soleil.fr

ISBN: 978-3-95450-262-2 ISSN: 2673-5350 doi: 10.18429/JACoW-IBIC2025-TUPMO17

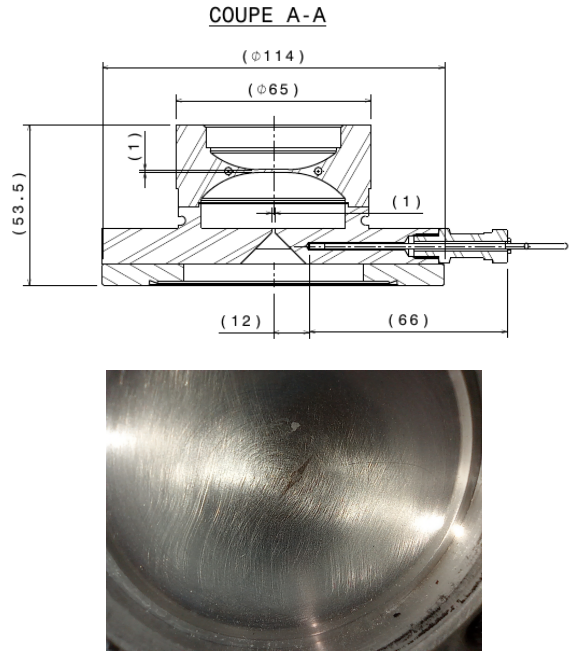

Figure 2: Aluminium UHV window installed on SOLEIL's PHCs: (top) 2D drawing, (bottom) picture of the exit face.

Several tests were performed to understand the origin of these structures. A first correlation was observed with the vertical emittance. As shown in Fig. 3, for emittances close to 200 pm·rad, the SR layer is perfectly smooth. However when the vertical emittance is reduced, filaments appear with an increasing contrast. At the minimum emittance, the contrast can reach 15 %. A second correlation was observed with the Copper filter thickness. For any given vertical emittance indeed, the filamented pattern can be blurred out by increasing the Copper filter thickness. The smaller is the emittance, the thicker has to be the Copper filter to reach the blurring. Several other parameters were varied but without any effect on the ending SR intensity distribution: the radio-frequency cavity voltage, the beam current and the filling pattern.

Since the filaments could be observed without Copper, both the Aluminium window and the imaging system were first suspected. However, systematic displacements of the imaging system and of the electron beam at source point (using orbit bumps) rapidly enabled to exclude the imaging system as the origin of the issue. After discussion with several beamline scientists, we finally understood that the filaments were in fact the result of a phase–contrast imaging of the Aluminium window.

Phase–contrast imaging is an imaging method using phase velocity alteration caused by refractive index variations, to resolve very small scale (sub–nm) structures. This technique, implemented by the way on several beamlines at SOLEIL, requires the use of an X-ray beam with a transverse coherence length smaller than the structure to be resolved. On the PHCs, the structured Aluminium window is imaged by phase–contrast on the ending scintillator. When the vertical emittance becomes small enough for the X–ray beam to reach a coherence length of the order of the Aluminium inner structures, these structures are imaged onto the scintillator. Because the vertical emittance is much smaller than the horizontal emittance, the transverse coherence is much larger in the vertical plane, which leads to this horizontal filamenting pattern. The filaments are blurred when a Copper filter is inserted on the X-ray path because the Copper hardens the X-ray beam spectrum, which reduces the transverse coherence length.

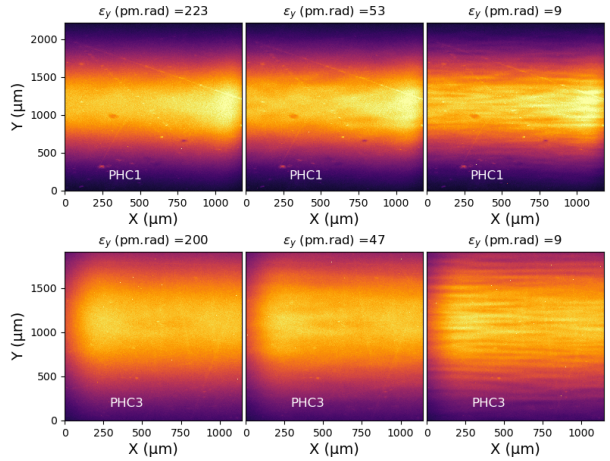

Figure 3: SR intensity distribution after 10 m of free propagation to the image plane versus electron beam vertical emittance. Data recorded on SOLEIL's PHCs (without pinhole) during dedicated machine studies.

These preliminary measurements therefore revealed an unexpected limitation in terms of performance of our exisiting PHCs: the building of filamented structures for vertical emittances below few tens of pm·rad. In the perspective of SOLEIL-II, with its reduced emittances in both planes, this issue has to be solved. Two solutions have been studied up to now: the use of a phase blurrer, or *decoherer*, and the use of different window materials.

TESTING OF A DECOHERER

The principle of a decoherer is to introduce a random phase variation along the SR path in order to destroy the coherence of the wavefront and therefore blur the filamented pattern. As done on some of SOLEIL beamlines, a high speed rotative axis (15 000 turns/minute) was then assembled, capable of holding Aluminium disks of different surface quality or Aluminium foams of different densities. An example of decoherer test is presented in Fig. 4. The SR intensity distribution is shown in (#0) with nothing but the PHC UHV window on its path, in (#1) with the decoherer installed but rotative axis switched off and in (#2) with the decoherer installed and the rotative axis set at maximum speed. In this case, it was an Aluminium foam of 3 mm thickness which was mounted on the rotative axis. However, whatever the material tested on the SR, it was impossible to blur out the filaments by more than a few percent.

ISBN: 978-3-95450-262-2 ISSN: 2673-5350 doi: 10.18429/JACoW-IBIC2025-TUPMO17

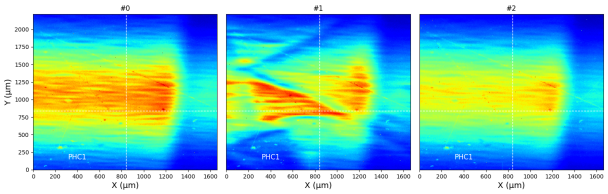

Figure 4: SR intensity distribution after PHC UHV window and 10 m of free propagation to the image plane : (#0) without decoherer, (#1) with decoherer but motor OFF and (#2) with decoherer and motor ON. The disk pounted on the rotative axis is an Aluminium foam of 3 mm thickness. Data recorded on SOLEIL's PHC1 beamline (without pinhole) during dedicated machine studies with $\epsilon_y = 9$ pm·rad.

TESTING OF DIFFERENT MATERIALS

The testing of different window materials was performed on the Metrology beamline of SOLEIL. This beamline has the same source point as the PHCs, i.e. one of the ring dipole. The beamline monochromator was removed to reproduce the conditions on the PHCs beamlines while a CVD window was used to ensure the vacuum-to-air transition. A imaging system similar to the one on the PHCs was installed at the end of the beamline. At the same distance upstream from the scintillator, a stage enabled to insert different materials on the X–ray path: a replica of the Aluminium window used on the PHC beamlines, as well as Aluminium foils of equivalent thicknesses (1 mm) but of different roughness. As shown in Fig. 5(a), when the PHC Aluminium window is introduced, highly contrasted speckles are observed with small vertical emittances, and these speckles partially blur with large vertical emittances. The structures observed are less alike filaments because, thanks to the larger distance from source to window, the transverse coherence especially in horizontal is larger. Introducing an Aluminium foil with a roughness of 0.05 µm, i.e. with a better surface quality, enables to reduce the contrast of the structures but not to remove them as shown in Fig. 5(b). However, leaving on the X-ray path nothing but the CVD window, the SR intensity distribution recovers its nominal homogeneity, even with the smallest vertical emittance as shown in Fig. 5(c). These experiments confirm the phase–contrast origin of the filaments observed on the PHCs but also reveal that the use of a CVD window might be mandatory on the PHCs of SOLEIL-II.

CONCLUSION

In the framework of SOLEIL-II, preliminary experiments were performed at SOLEIL to pinpoint the resolution limits of the existing pinhole cameras ensuring the emittance measurements. While reducing the vertical emittance below 50 pm·rad, a filamentation was observed in the intensity distribution of the SR emitted by the source dipole in the image plane. This filamentation significantly affects the emittance measurement, introducing in particular a parasitic orbit dependency. This filamentation revealed to correspond to the phase–contrast imaging of the Aluminium UHV window of the PHCs. To get rid of this effect, the use of a decoherer and of better surface quality Aluminium windows were attempted, however without success. This work reveals that the use of a CVD window for the vacuum-to-air transition on the PHCs might be mandatory to ensure high resolution emittance measurements on SOLEIL-II storage ring.

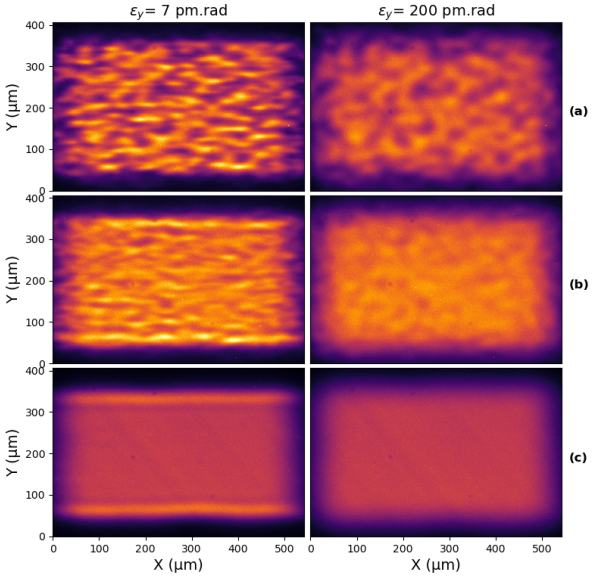

Figure 5: SR intensity distribution after 20 m of free propagation to the image plane versus electron beam vertical emittance and through different Aluminium materials: (a) PHC UHV window, (b) 1 mm thick Aluminium window with roughness 0.05 µm, (c) no Aluminiuum window. Data recorded on Metrology's beamline using a CVD window for vacuum to air transition at 15 m from source point.

REFERENCES

[1] P. Elleaume, C. Fortgang, C. Penel, and E. Tarazona, "Measuring Beam Sizes and Ultra-Small Electron Emittances Using an X-ray Pinhole Camera", *J. Synchrotron Radiat.*, vol. 2, no. 5, pp. 209–214, Sep. 1995. doi:10.1107/s0909049595008685

[2] M.-A. Tordeux, L. Cassinari, O. V. Chubar, J.-C. Denard, D. Pedeau, and B. Pottin, "Ultimate Resolution of Soleil X-Ray Pinhole Camera", in *Proc. DIPAC'07*, Venice, Italy, May 2007, paper TUPC16, pp. 180–182.

[3] O. Chubar and P. Elleaume, "Accurate and Efficient Computation of Synchrotron Radiation in the Near Field Region", in *Proc. EPAC'98*, Stockholm, Sweden, Jun. 1998, paper THP01G, pp. 1177–1179.